

Third-order aberration coefficients of the Fraunhofer hologram formed at spherical surface of the recording medium

EUGENIUSZ JAGOSZEWSKI

Institute of Physics, Technical University of Wrocław, Wybrzeże Wyspiańskiego 27,
50-370 Wrocław, Poland.

1. Introduction

The aberrations of reconstructed images in holography are given as a function of the object, reference and reconstruction coordinates, as well as the wavelength ratio and the scale factor of hologram [1-6]. In the case of a non-plane hologram, for example, in a hologram with the basis of spherical shape, the aberrations depend also upon the curvature of its surface [7-15]. In this paper the expression for third-order aberrations in the wavefronts reconstructed from Fraunhofer hologram made at spherical surface are derived, and the influence of the hologram curvature on the aberrations is shown.

Like in paper [16] let us consider first an object point P_0 in Cartesian coordinate system whose origin is at the vertex of the spherical hologram surface with a centre on z -axis. When a spherical wave emerges from the object, reference or reconstruction point source, then its phase within the spherical surface of the recording medium (hologram) related to the phase at the vertex is given by

$$\begin{aligned}\Phi_0(x, y, z) &= k_1(r_0 - R_0), \\ \Phi_R(x, y, z) &= k_1(r_R - R_R), \\ \Phi_C(x, y, z) &= k_2(r_C - R_C),\end{aligned}$$

respectively, $k_1 = 2\pi/\lambda_1$ and $k_2 = 2\pi/\lambda_2$ being the wavenumber. If the points $P(x, y, z)$ of the spherical surface are described in spherical coordinates: $P(\varrho, \Theta, \varphi)$, then the expansion of the square roots in the phase expression yields

$$\begin{aligned}\Phi_N(\varrho, \Theta, \varphi) &= \frac{k_{1,2}}{2z_N} \left[4\varrho^2 \sin^2 \left(\frac{\Theta}{2} \right) \left(1 + \frac{z_N}{\varrho} \right) - 2\varrho \sin \Theta (x_N \cos \varphi + y_N \sin \varphi) \right] \\ &\quad - \frac{k_{1,2}}{8z_N^3} \left[16\varrho^4 \sin^4 \left(\frac{\Theta}{2} \right) \left(1 + \frac{z_N}{\varrho} \right)^2 - 16\varrho^3 \sin \Theta \sin^2 \left(\frac{\Theta}{2} \right) \left(1 + \frac{z_N}{\varrho} \right) \right. \\ &\quad \times (x_N \cos \varphi + y_N \sin \varphi) + 4\varrho^2 \sin^2 \Theta (x_N^2 \cos^2 \varphi + y_N^2 \sin^2 \varphi) \\ &\quad \left. + x_N y_N \sin 2\varphi \right] + 8(x_N^2 + y_N^2) \left(1 + \frac{z_N}{\varrho} \right) \varrho^2 \sin^2 \left(\frac{\Theta}{2} \right) - 4(x_N^2 + y_N^2) \\ &\quad \left. (x_N \cos \varphi + y_N \sin \varphi) \varrho \sin \Theta \right] \quad (1)\end{aligned}$$

where $N = O, R, C, I$ for object, reference, reconstruction and image wave, respectively. By adding the phases of all wavefronts the participating in recording and reconstruction processes, the phase of the two reconstructed waves can be calculated from the equation

$$k_2 \Delta r_I = k_2 (r_I - R_I) = k_2 \Delta r_C \pm k_1 (\Delta r_O - \Delta r_R) - \Phi_{AB} \quad (2)$$

where Φ_{AB} represents the wavefront aberrations, defined as the phase difference between the Gaussian reference sphere and the actual wavefront created during illumination of the hologram surface. Assuming $(x_N^2 + y_N^2)/\lambda \ll z_N$, and $x, y \ll z_N$ for the Fraunhofer hologram (Fig. 1), the first approximation of Eq. (2) provides ($\Phi_{AB} = 0$) the paraxial imaging equations

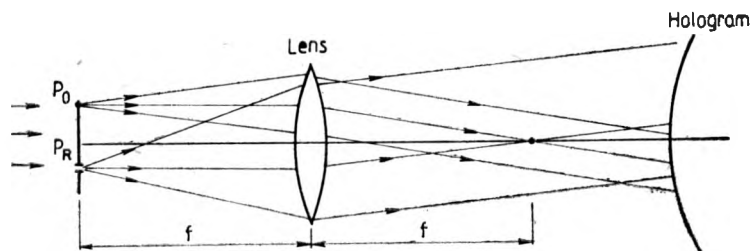


Fig. 1. Formation of a Fraunhofer hologram at a spherical surface

$$\begin{aligned} z_I &= z_C, \\ \sin \alpha_I &= \sin \alpha_C \pm \mu (\sin \alpha_O - \sin \alpha_R), \\ \sin \beta_I &= \sin \beta_C \pm \mu (\sin \beta_O - \sin \beta_R) \end{aligned} \quad (3)$$

where $\mu = \lambda_2/\lambda_1$ and α_N, β_N are the angles between z -axis and suitable directions of ray projection at (x, z) - and (y, z) -plane, respectively.

2. Third-order aberration coefficients

By the subsequent approximation of Eq. (2) and when the above conditions are fulfilled, we have $\Phi_{AB} \neq 0$ and the third-order aberration coefficients [16] for a Fraunhofer hologram formed on the spherical surface are given by

$$\begin{aligned} S &= \frac{1}{z_C^3} - \frac{1}{z_I^3} + \frac{2}{\rho} \left(\frac{1}{z_C^2} - \frac{1}{z_I^2} \right) + \frac{1}{\rho^2} \left(\frac{1}{z_C} - \frac{1}{z_I} \right), \\ C_x &= \frac{\sin \alpha_C}{z_C^2} - \frac{\sin \alpha_I}{z_I^2} + \frac{1}{\rho} \left(\frac{\sin \alpha_C}{z_C} - \frac{\sin \alpha_I}{z_I} \right), \\ C_y &= \frac{\sin \beta_C}{z_C^2} - \frac{\sin \beta_I}{z_I^2} + \frac{1}{\rho} \left(\frac{\sin \beta_C}{z_C} - \frac{\sin \beta_I}{z_I} \right), \\ A_x &= \frac{\sin^2 \alpha_C}{z_C} - \frac{\sin^2 \alpha_I}{z_I}, \end{aligned} \quad (4)$$

$$\begin{aligned}
 A_y &= \frac{\sin^2 \beta_C}{z_C} - \frac{\sin^2 \beta_I}{z_I}, \\
 A_{xy} &= \frac{\sin \alpha_C \sin \beta_C}{z_C} - \frac{\sin \alpha_I \sin \beta_I}{z_I}, \\
 F &= \frac{1}{z_C} (\sin^2 \alpha_C + \sin^2 \beta_C) - \frac{1}{z_I} (\sin^2 \alpha_I + \sin^2 \beta_I) + \frac{1}{\varrho} (\sin^2 \alpha_C + \sin^2 \beta_C \\
 &\quad - \sin^2 \alpha_I - \sin^2 \beta_I),
 \end{aligned} \tag{4}$$

$$D_x = (\sin^2 \alpha_C + \sin^2 \beta_C) \sin \alpha_C - (\sin^2 \alpha_I + \sin^2 \beta_I) \sin \alpha_I,$$

$$D_y = (\sin^2 \alpha_C + \sin^2 \beta_C) \sin \beta_C - (\sin^2 \alpha_I + \sin^2 \beta_I) \sin \beta_I.$$

As was shown in paper [16], only a spherical aberration, coma and field curvature depend on the curvature of the hologram surface. In a special case, by using the paraxial imaging Eqs. (3), we get the aberration coefficients in simple form, namely:

$$S = 0,$$

$$C_x = \frac{1}{z_C} \left(\frac{1}{z_C} + \frac{1}{\varrho} \right) (\sin \alpha_C - \sin \alpha_I),$$

$$C_y = \frac{1}{z_C} \left(\frac{1}{z_C} + \frac{1}{\varrho} \right) (\sin \beta_C - \sin \beta_I),$$

$$A_x = \frac{1}{z_C} (\sin^2 \alpha_C - \sin^2 \alpha_I),$$

$$A_y = \frac{1}{z_C} (\sin^2 \beta_C - \sin^2 \beta_I),$$

$$A_{xy} = \frac{1}{z_C} (\sin \alpha_C \sin \beta_C - \sin \alpha_I \sin \beta_I),$$

$$F = \left(\frac{1}{z_C} + \frac{1}{\varrho} \right) (\sin^2 \alpha_C + \sin^2 \beta_C - \sin^2 \alpha_I - \sin^2 \beta_I);$$

the distortion coefficients being the same as in Eqs. (4). We see that the spherical aberration always disappears, since for the Fraunhofer hologram $z_I = z_C$. We can also see that when a reconstruction point source is situated at a distance $z_C = -\varrho$, coma and field curvature will be eliminated simultaneously. Thus, when a Fraunhofer hologram is formed on a spherical surface of the recording medium for the two images the spherical aberration, coma and field curvature can be made to disappear simultaneously by using the reconstruction beam point source. In this situation, all the aberrations do not depend on the wavelength ratio.

3. Lensless Fraunhofer hologram

In the case where the reference-beam source on the optical axis is at infinity and the object at the finite distance from the surface of the recording medium, a lensless Fraunhofer hologram (Fig. 2) is obtained. THOMPSON [17], JAGOSZEWSKI and PAWLUK [18] employed this method to measure the size and shape of dynamic aerosol particles, but at the plane surface. A Fraunhofer hologram formed by illuminating an object surface with plane coherent wave, when the recording surface is placed in a far-field distance from the object.

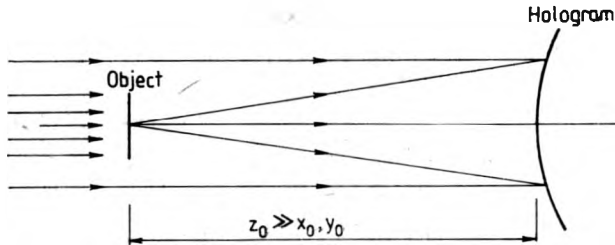


Fig. 2. Formation of a lensless Fraunhofer hologram at a spherical surface

In this case, due to small skewness (α_C, β_C) of the reconstruction beam the paraxial Eqs. (3) take the forms

$$\begin{aligned} \frac{1}{z_I} &= \frac{1}{z_C} \pm \frac{\mu}{z_O}, \\ \sin \alpha_I &= \sin \alpha_C \pm \mu \sin \alpha_O, \\ \sin \beta_I &= \sin \beta_C \pm \mu \sin \beta_O, \end{aligned} \quad (5)$$

and the third-order aberration coefficients [16] are as follows:

$$\begin{aligned} S &= \frac{1}{z_C^3} - \frac{1}{z_I^3} \pm \frac{\mu}{z_O^3} + \frac{2}{\rho} \left(\frac{1}{z_C^2} - \frac{1}{z_I^2} \pm \frac{\mu}{z_O^2} \right), \\ C_x &= \frac{\sin \alpha_C}{z_C^2} - \frac{\sin \alpha_I}{z_I^2} \pm \frac{\mu \sin \alpha_O}{z_O^2} + \frac{1}{\rho} \left(\frac{\sin \alpha_C}{z_C} - \frac{\sin \alpha_I}{z_I} \pm \frac{\mu \sin \alpha_O}{z_O} \right), \\ C_y &= \frac{\sin \beta_C}{z_C^2} - \frac{\sin \beta_I}{z_I^2} \pm \frac{\mu \sin \beta_O}{z_O^2} + \frac{1}{\rho} \left(\frac{\sin \beta_C}{z_C} - \frac{\sin \beta_I}{z_I} \pm \frac{\mu \sin \beta_O}{z_O} \right), \\ A_x &= \frac{\sin^2 \alpha_C}{z_C} - \frac{\sin^2 \alpha_I}{z_I} \pm \frac{\mu \sin^2 \alpha_O}{z_O}, \\ A_y &= \frac{\sin^2 \beta_C}{z_C} - \frac{\sin^2 \beta_I}{z_I} \pm \frac{\mu \sin^2 \beta_O}{z_O}, \\ A_{xy} &= \frac{\sin \alpha_C \sin \beta_C}{z_C} - \frac{\sin \alpha_I \sin \beta_I}{z_I} \pm \frac{\mu \sin \alpha_O \sin \beta_O}{z_O}, \end{aligned} \quad (6)$$

$$\begin{aligned}
 F &= \frac{1}{z_C} (\sin^2 \alpha_C + \sin^2 \beta_C) - \frac{1}{z_I} (\sin^2 \alpha_I + \sin^2 \beta_I) \pm \frac{\mu}{z_O} (\sin^2 \alpha_O + \sin^2 \beta_O) \\
 &\quad + \frac{1}{\rho} [\sin^2 \alpha_C + \sin^2 \beta_C - \sin^2 \alpha_I - \sin^2 \beta_I \pm \mu (\sin^2 \alpha_O + \sin^2 \beta_O)], \\
 D_x &= (\sin^2 \alpha_C + \sin^2 \beta_C) \sin \alpha_C - (\sin^2 \alpha_I + \sin^2 \beta_I) \sin \alpha_I \pm \mu (\sin^2 \alpha_O \\
 &\quad + \sin^2 \beta_O) \sin \alpha_O, \\
 D_y &= (\sin^2 \alpha_C + \sin^2 \beta_C) \sin \beta_C - (\sin^2 \alpha_I + \sin^2 \beta_I) \sin \beta_I \\
 &\quad \pm \mu (\sin^2 \alpha_O + \sin^2 \beta_O) \sin \beta_O.
 \end{aligned} \tag{6}$$

In contradistinction to the Fraunhofer hologram formed by a lens, the aberrations of the lensless Fraunhofer hologram depend also on the wavelength ratio. The aberrations of the Fraunhofer hologram can be also eliminated by the plane, and partially by the spherical illuminating wave. If $\mu = 1$ and $z_C = z_O$, then one image is placed at the finite distance ($z_I = z_O/2$) from the hologram, and the other one at infinity ($z_I = \infty$). Thus, for the primary image we have:

$$\begin{aligned}
 S &= -\frac{2}{z_O^2} \left(\frac{3}{z_O} + \frac{2}{\rho} \right), \\
 C_x &= -\frac{1}{z_O} \left(\frac{3}{z_O} + \frac{1}{\rho} \right) (\sin \alpha_C + \sin \alpha_O), \\
 C_y &= -\frac{1}{z_O} \left(\frac{3}{z_O} + \frac{1}{\rho} \right) (\sin \beta_C + \sin \beta_O), \\
 A_x &= -\frac{1}{z_O} [(\sin \alpha_C + \sin \alpha_O)^2 + 2 \sin \alpha_C \sin \alpha_O], \\
 A_y &= -\frac{1}{z_O} [(\sin \beta_C + \sin \beta_O)^2 + 2 \sin \beta_C \sin \beta_O], \\
 A_{xy} &= -\frac{1}{z_O} [\sin \beta_O (\sin \alpha_O + 2 \sin \alpha_C) + \sin \beta_C (\sin \alpha_C + 2 \sin \alpha_O)], \\
 F &= -\frac{1}{z_O} [(\sin \alpha_C + \sin \alpha_O)^2 + (\sin \beta_C + \sin \beta_O)^2] \\
 &\quad - 2 \left(\frac{1}{z_O} + \frac{1}{\rho} \right) (\sin \alpha_C \sin \alpha_O + \sin \beta_C \sin \beta_O), \\
 D_x &= -\sin \alpha_C (3 \sin^2 \alpha_O + \sin^2 \beta_O) - \sin \alpha_O (3 \sin^2 \alpha_C + \sin^2 \beta_C) \\
 &\quad - 2 \sin \beta_C \sin \beta_O (\sin \alpha_C + \sin \alpha_O), \\
 D_y &= -\sin \beta_C (3 \sin^2 \beta_O + \sin^2 \alpha_O) - \sin \beta_O (3 \sin^2 \beta_C + \sin^2 \alpha_C) \\
 &\quad - 2 \sin \alpha_C \sin \alpha_O (\sin \beta_C + \sin \beta_O).
 \end{aligned} \tag{7}$$

And for the secondary image

$$\begin{aligned}
 S &= 0, \\
 C_x &= \frac{1}{z_0} \left(\frac{1}{z_0} - \frac{1}{\rho} \right) (\sin \alpha_C - \sin \alpha_0), \\
 C_y &= \frac{1}{z_0} \left(\frac{1}{z_0} - \frac{1}{\rho} \right) (\sin \beta_C - \sin \beta_0), \\
 A_x &= \frac{1}{z_0} (\sin^2 \alpha_C - \sin^2 \alpha_0), \\
 A_y &= \frac{1}{z_0} (\sin^2 \beta_C - \sin^2 \beta_0), \\
 A_{xy} &= \frac{1}{z_0} (\sin \alpha_C \sin \beta_C - \sin \alpha_0 \sin \beta_0), \\
 F &= \frac{1}{z_0} (\sin^2 \alpha_C + \sin^2 \beta_C) + \frac{2}{\rho} (\sin \alpha_C \sin \alpha_0 + \sin \beta_C \sin \beta_0) \\
 &\quad - \left(\frac{1}{z_0} + \frac{2}{\rho} \right) (\sin^2 \alpha_0 + \sin^2 \beta_0).
 \end{aligned} \tag{8}$$

Coefficients D_x , D_y are the same as in expressions (7).

4. Final remarks

Considerations over the quality of reconstructed images from the Fraunhofer holograms lead to conclusions that all the aberrations can be eliminated by using a plane illuminating wave during the reconstruction process. By using a spherical illuminating wave only some aberrations can be eliminated, the more so, when the hologram is formed at the nonplane surface.

References

- [1] MEIER W. W., J. Opt. Soc. Am. **55** (1965), 987.
- [2] CHAMPAGNE E. B., J. Opt. Soc. Am. **57** (1967), 51.
- [3] LATA J. N., Appl. Opt. **10** (1971), 599.
- [4] Ibidem, p. 609.
- [5] Ibidem, p. 2698.
- [6] MILES J. F., Optica Acta **19** (1972), 165.
- [7] MUSTAFIN K. S., Optika i Spektr. **37** (1974), 1158.
- [8] WELFORD W. T., Opt. Commun. **8** (1973), 239.
- [9] Ibidem, **15** (1975), 46.
- [10] WELFORD W. T., J. Phot. Sc. **23** (1975), 84.
- [11] SWEAT W. C., J. Opt. Soc. Am. **67** (1977), 803.
- [12] SMITH R. W., Opt. Commun. **21** (1977), 102.

- [13] Ibidem, p. 106.
- [14] NOWAK J., *Optica Applicata* **10** (1980), 245.
- [15] PENG KE-OU, *Imaging by Curved Holographic Optical Elements*, Doctor's Thesis, Delft University, Dutch Efficiency Bureau-Pijnacker, 1983.
- [16] JAGOSZEWSKI E., *The influence of the hologram surface curvature on the holographic imaging quality*, *Optik*, in press.
- [17] THOMPSON B. J., WARD J. H., ZINKY W., *Appl. Opt.* **6** (1967), 519.
- [18] JAGOSZEWSKI E., PAWLUK T., *Optica Applicata* **10** (1980), 399.

*Received August 30, 1984,
in revised form October 8, 1984*